Correction Mechanism Analysis for a Class of Spin-stabilized Projectile with Fixed Canards

Yi Wang, Wei-dong Song, Qing-wei Guo, Xie-en Song, Gang Wang

Abstract—**Correction control mechanism for a class of spin-stabilized projectile is presented. The analyzed configuration couples correction part and the body part, and the correction part with fixed canards and sensors aims at trajectory correction. Formulas of the dynamic equilibrium angle and drift are derived, and by integrating the deviation motion along the trajectory the drift value can be obtained. The analytic solution of the deviation motion is acquired, and it points out that the dynamic equilibrium angle induced by trajectory correction is the key factor. Through studying the influence of correction to the dynamic equilibrium angle and attack angle, the correction mechanism is found. Simulation results show that the components of control angle in the vertical and horizontal planes make the projectile axis move to the components' opposite directions, and produce negative correction control effect.**

Index Terms—**correction mechanism, equation of attack angle, dynamic equilibrium angle, drift, spin-stability projectile**

I. INTRODUCTION

GUIDED artillery projectiles have attracted increasing interests over last few decades because of the hgigh

Yi Wang is with Shijiazhuang Mechanical Engineering College, Shijiazhuang 050003, China (corresponding author phone: +861508873291; e-mail: wangyi050926@163.com).

Wei-dong Song, is with Shijiazhuang Mechanical Engineering College, Shijiazhuang 050003, China (e-mail: wdsung@163. com).

Qing-wei Guo is with Shijiazhuang Mechanical Engineering College, Shijiazhuang 050003, China (e-mail: gqingwei@sina.cn).

Xie-en Song is with Shijiazhuang Mechanical Engineering College, Shijiazhuang 050003, China (e-mail: songxieen1988@163. com).

Gang Wang is with Shijiazhuang Mechanical Engineering College, Shijiazhuang 050003, China (e-mail: g_wang@foxmail.com).

delivery accuracy and decreasing dispersion requirements. Since more sensors and control actuators are involved in, more complex configurations need to be considered to deal with the conflict between the conventional projectile design and new requirements. Dual spin configuration is a very appropriate choice to achieve two-dimension trajectory correction, and the conventional projectiles can be simply retrofitted by replacing the fuse, so this method is considered to be the best one to make the old projectiles have new lives.

In the last few years, the dual spin configuration has been studied extensively, and some dual spin aircrafts have arisen. Regan and Smith took dual spin configuration into spin projectiles for trajectory correction, and proved the effectiveness in the terminal course correction [1]. Then US naval air warfare center studied the guidance integrated fuse (GIF) [2]. Alliant Techsystems (ATK) produced the Precision Guidance Kit (PGK) and the Mortar Guidance Kit (MGK), and the two have been armed in the US army. Gagnon and Lauzon compared PGK with course correction fuse (CCF), and they pointed out the advantages of the two, respectively [3]. Werent proposed a new design which used a set of fixed canards to control the front part to reduce the roll velocity and used a set of reciprocating canards to correct the course [4]. Wernert and Theodoulis changed the design, and the set of fixed canards was replaced by a set of reciprocating canards [5]. Wang and Shi presented another scheme, and a damping disk and damping rings were taken, which were used for longitudinal and lateral correction [6].

Because of high reliability, taking small volume and supplying continuous loads, trajectory correction fuse with fixed canards has aroused increasing interest among researchers. Costello established 7-freedom rigid trajectory model [7], and he linearized the model to research the stability of projectiles [8]. Ji and Zhang studied the aerodynamics [9-10]. Li established a course model for

122mm rockets and analyzed the stability [11]. Toledo introduced the experiment method for a kind of 120 mm mortar ammunition [12]. However, to our best knowledge there is no literature introducing the trajectory characteristics of spin-stabilized projectiles during the course correction periods, especially the correction mechanism.

This work deals with the research on the correction mechanism of the spin-stabilized projectiles. The dynamic model under control state is established in Sec. II, and equation of attack angle and formula of dynamic equilibrium angle are deduced in Sec. III. Based on the formulas, deviation motion of the trajectory and the correction control mechanism are analyzed in Sec. IV. Simulation results are provided to show how the correction control affects the impact points through controlling motions of projectile axis in Sec. V. Finally, conclusions are presented in Sec. VI.

II. DYNAMIC MODEL

The trajectory correction fuse with fixed canards comprises of front and aft components, and the two components are connected by two bearings (as is shown in Fig. 1), which allows them spin in different directions. On the aft component there is a screw thread, using which the fuse can be fitted into the projectile. After the fuse is fitted, the projectile can be divided into two parts. One is named correction part, and the other is named body part.
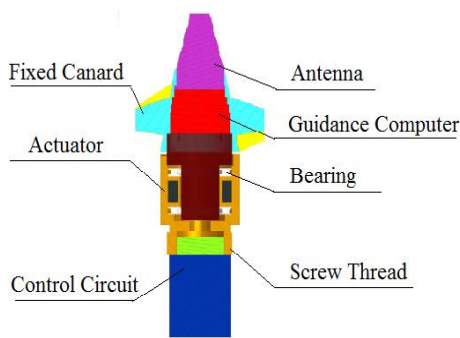
a) Structure of the fuse

b) Schematic of the installation

Fig. 1. Two dimension course correction fuses

During the flight, the two parts of the projectile spin in different directions due to the effort of the aerodynamic forces. In order to describe the motion of the projectile, three translational and four rotational rigid body degrees of freedom are introduced. The translational degrees of freedom are the three components of the mass center position vector. The rotational degrees of freedom are the Euler yaw and pitch angles as well as the correction part roll and body part roll angles. The ground surface is used as an inertial reference frame, which is named $oxyz$.

The quasi body reference frame $ox_4y_4z_4$ is introduced to describe the rotational motion (as is shown in Fig. 2), and the sequence of rotation from the inertial frame is pitch φ, yaw ψ. The ox_4y_4 plane of the quasi body reference frame is fixed in the vertical plane, so it is convenient to be shared by the correction part and body part.
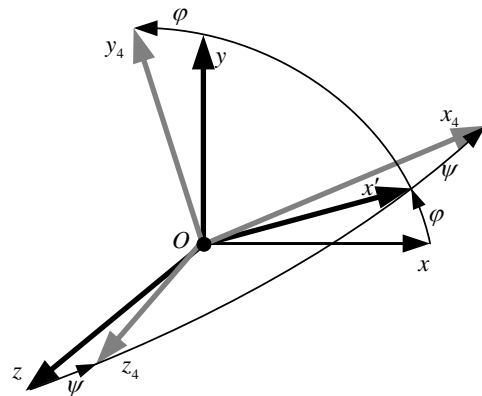

Fig. 2. Coordinate transformation relation

Equations (1-4) represent the translational and rotational equations of motion for a dual spin projectile. Both sets of translational equations are expressed in the inertial frame:

$$\begin{bmatrix} \dot{v}_x \\ \dot{v}_y \\ \dot{v}_z \end{bmatrix} + \begin{bmatrix} 0 & \omega_{z4} & -\omega_{y4} \\ \omega_{z4} & 0 & \omega_{z4}\tan\psi \\ -\omega_{y4} & -\omega_{z4}\tan\psi & 0 \end{bmatrix} \begin{bmatrix} v_x \\ v_y \\ v_z \end{bmatrix} = \frac{1}{m}\begin{bmatrix} F_x \\ F_y \\ F_z \end{bmatrix} + \begin{bmatrix} g_x \\ g_y \\ g_z \end{bmatrix},$$

(1)

$$\begin{bmatrix} \dot{x} \\ \dot{y} \\ \dot{z} \end{bmatrix} = \begin{bmatrix} v_x \\ v_y \\ v_z \end{bmatrix}.$$

(2)

F_x, F_y and F_z are components of the total force expressed in the inertial frame. v_x, v_y and v_z are velocity vector components of the composite center of mass expressed in the inertial frame. x, y and z are position vector

components of the composite center of mass expressed in the inertial frame. ω_{y4} and ω_{z4} are components of the angular velocity vector expressed on the y and z axis of the quasi body reference frame.

The two rotational equations are expressed in the quasi body reference frame:

$$\begin{bmatrix} J_{xh}\dot{\omega}_{xf} \\ J_x\dot{\omega}_{x4} \\ J_y\dot{\omega}_{y4} \\ J_z\dot{\omega}_{z4} \end{bmatrix} = \begin{bmatrix} M_{xf} \\ M_x \\ M_y \\ M_z \end{bmatrix} - \begin{bmatrix} 0 \\ (J_z - J_y)\omega_{y4}\omega_{z4} \\ (J_x - J_z)\omega_{x4}\omega_{z4} \\ (J_y - J_x)\omega_{x4}\omega_{y4} \end{bmatrix} + \begin{bmatrix} 0 \\ 0 \\ -J_z\omega_{z4}\dot{\gamma}_a \\ J_y\omega_{y4}\dot{\gamma}_a \end{bmatrix}, \quad (3)$$

$$\begin{bmatrix} \dot{\varphi} \\ \dot{\psi} \\ \dot{\gamma}_a \\ \dot{\gamma}_f \end{bmatrix} = \begin{bmatrix} 0 & \sin\gamma/\cos\psi & \cos\gamma_\gamma/\cos\psi & 0 \\ 0 & \cos\gamma_a & -\sin\gamma_a & 0 \\ 1 & \tan\psi\sin\gamma_a & \tan\psi\cos\gamma_a & 0 \\ 0 & 0 & 0 & 1 \end{bmatrix} \begin{bmatrix} \omega_{x4} \\ \omega_{y4} \\ \omega_{z4} \\ \omega_{xf} \end{bmatrix}. \quad (4)$$

M_{xf}, M_x, M_y and M_z are components of the total moment of both the front and aft parts expressed on the x axis of the quasi body reference frame. γ_f, γ_a are roll angles of the front and aft part. ψ, φ are yaw angle and pitch angle, respectively.

Loads on the composite projectile body are due to weight and aerodynamic forces. All the aerodynamic coefficients are acquired by numerical computing, and the forces as well as moments are presented as follows:

$$\begin{cases} F_{x4} = -\dfrac{1}{2}\rho v^2 SC_a \ , \\[2mm] F_{y4} = \dfrac{1}{2}\rho v^2 SC_n'\alpha - \dfrac{1}{2}\rho v^2 SC_{zf}''\dfrac{d\dot{\gamma}_f}{v}\beta \ , \\[2mm] -\dfrac{1}{2}\rho v^2 SC_{za}''\dfrac{d\dot{\gamma}_a}{v}\beta + \dfrac{1}{2}\rho v^2 SC_{n\delta}\left(\delta_z c_{\gamma_f} + \alpha\right) \ , \\[2mm] F_{z4} = -\dfrac{1}{2}\rho v^2 SC_n'\beta - \dfrac{1}{2}\rho v^2 SC_{zf}''\dfrac{d\dot{\gamma}_f}{v}\alpha \\[2mm] -\dfrac{1}{2}\rho v^2 SC_{za}''\dfrac{d\dot{\gamma}_a}{v}\alpha - \dfrac{1}{2}\rho v^2 SC_{n\delta}\left(-\delta_z s_{\gamma_f} + \beta\right) \ . \end{cases}$$

$$\begin{cases} M_{xf} = \dfrac{1}{2}\rho v^2 SLm_{xh} - \dfrac{1}{2}\rho v^2 SL\dfrac{dp_f}{v}C_{lpf} - M_{fa} \ , \\[2mm] M_x = -\dfrac{1}{2}\rho v^2 SL\dfrac{dp_a}{v}C_{lpa} - M_{af} \ , \\[2mm] M_y = \dfrac{1}{2}\rho v^2 SLm_z'\beta - \dfrac{1}{2}\rho v^2 SLC_{nr}\dfrac{Lr}{v} + \dfrac{1}{2}\rho v^2 SLC_{npaf}\dfrac{d\dot{\gamma}_f}{v}\alpha \\[2mm] +\dfrac{1}{2}\rho v^2 SLC_{npaa}\dfrac{d\dot{\gamma}_a}{v}\alpha + \dfrac{1}{2}\rho v^2 SL_C C_{n\delta}\left(-\delta_z c_{\gamma_f} + \beta\right) \ , \\[2mm] M_z = \dfrac{1}{2}\rho v^2 SLm_z'\alpha - \dfrac{1}{2}\rho v^2 SLC_{mq}\dfrac{Lq}{v} - \dfrac{1}{2}\rho v^2 SLC_{npaf}\dfrac{d\dot{\gamma}_f}{v}\beta \\[2mm] -\dfrac{1}{2}\rho v^2 SLC_{npaa}\dfrac{d\dot{\gamma}_a}{v}\beta + \dfrac{1}{2}\rho v^2 SL_C C_{n\delta}\left(\delta_z s_{\gamma_f} + \alpha\right) \ . \end{cases}$$

Note that the force vector $\begin{bmatrix} F_{x4} & F_{y4} & F_{z4} \end{bmatrix}^T$ presents the components of aerodynamic forces in the quasi body reference frame, and it should be transformed into a vector in the inertial frame. The longitudinal and lateral aerodynamic angles of attack are computed as follows:

$$\alpha = \tan^{-1}\left(\frac{-v_{y4}}{v}\right), \quad \beta = \tan^{-1}\left(\frac{v_{z4}}{v}\right) \ . \quad (5)$$

When in the trajectory correction process, correction part is set to a roll angle relative to the inertial frame, so the control relationship is added as follows:

$$\begin{cases} \gamma_f = \gamma_c \\ \dot{\gamma}_f = p_f = 0 \end{cases} \ . \quad (6)$$

III. DYNAMIC EQUILIBRIUM ANGLE

The projectile system is a nonlinear time varying system. That is to say, all the aerodynamic coefficients and kinematic parameters change as time goes on. Here coefficients frozen method is taken for formula deduction. In order to describe the motion of angles, the equations of attack angles need to be established, and some assumptions are invoked:

1) The attack and sideslip angles are small in the flight, so that

$$\alpha \approx -\frac{v_{y4}}{v} \ , \quad \beta \approx \frac{v_{z4}}{v} \ . \quad (7)$$

2) Compared to v_{x4}, ω_{x4} and ω_{xh}, the quantities ω_{y4}, ω_{z4}, v_{y4} and v_{z4} are small, so that the total velocity

$$\dot{v} \approx \dot{v}_{x4} = -\frac{\rho SC_a}{2m}v^2 - g\sin\varphi\cos\psi \ . \quad (8)$$

Products of small quantities and their derivatives are negligible.

3) The variables are changed from time t to arclength s, and have units of calibers of travel:

$$s = \int_0^t v \, d\tau \ . \quad (9)$$

4) The projectile is mass balanced, such that the centers of gravity of both the correction part and body part lie on the rotational axis of symmetry:

$$J_z = J_y \ .$$

A. Equation of Attack Angles

Neglecting the products of small quantities, the derivation of (7) is that

$$\dot{\alpha} = -\frac{F_{y4}}{mv} + \omega_{z4} - \frac{\dot{v}}{v}\alpha \ , \quad \dot{\beta} = \frac{F_{z4}}{mv} + \omega_{y4} - \frac{\dot{v}}{v}\beta \ .$$

Let $\Delta = \alpha - i\beta, \mu = r + iq, J_y = J_z = A$, the equation of attack angles is acquired:

$$\Delta'' + (H - iP)\Delta' - (M + iPT)\Delta = G + D \quad . \qquad (10)$$

G and D are the gravity term and control force term respectively, and the meaning of the symbols are as follows:

$$H = k_{zz} + b_y - b_x - \frac{g}{v^2} s_\varphi c_\psi + b_c,$$

$$P = \frac{b_{zf}\dot{\gamma}_f + b_{za}\dot{\gamma}_a}{v} + \frac{J_{xf}\dot{\gamma}_f + J_{xa}\dot{\gamma}_a}{Av} \quad,$$

$$M = k_z - k_{zz}\left(b_y - b_x - \frac{g}{v^2} s_\varphi c_\psi + b_c\right)$$

$$+ \frac{(J_{xf}\dot{\gamma}_f + J_{xa}\dot{\gamma}_a)(b_{zf}\dot{\gamma}_f + b_{za}\dot{\gamma}_a)}{Av^2} + k_c \quad,$$

$$PT = \frac{J_{xf}\dot{\gamma}_f + J_{xa}\dot{\gamma}_a}{Av}\left(b_y - b_x - \frac{g}{v^2} s_\varphi c_\psi + b_c\right)$$

$$+ \frac{k_{zz}(b_{zf}\dot{\gamma}_f + b_{za}\dot{\gamma}_a)}{v} - \frac{(k_{yf}\dot{\gamma}_f + k_{ya}\dot{\gamma}_a)}{v} \quad,$$

$$G = \frac{g}{v^2}(c_\varphi + i s_\varphi s_\psi)\left(k_{zz} - i\frac{J_{xf}\dot{\gamma}_f + J_{xa}\dot{\gamma}_a}{Av}\right),$$

$$D = \left[k_c - b_c\left(k_{zz} - i\frac{J_{xf}\dot{\gamma}_f + J_{xa}\dot{\gamma}_a}{Av}\right)\right]\delta_z e^{i\gamma_f} \quad.$$

$$b_x = \frac{\rho S C_a}{2m}, \quad b_y = \frac{\rho S C_n'}{2m}, \quad b_{zf} = \frac{\rho S d C_{zf}''}{2m},$$

$$b_{za} = \frac{\rho S d C_{za}''}{2m}, \quad b_c = \frac{\rho S C_{n\delta}}{2m}, \quad k_z = \frac{\rho S L m_z'}{2A},$$

$$k_{zz} = \frac{\rho S L^2 C_{mq}}{2A}, k_{yf} = \frac{\rho S L d C_{npaf}}{2A}, k_c = \frac{\rho S L_c C_{n\delta}}{2A},$$

$$k_{ya} = \frac{\rho S L d C_{npaa}}{2A} \quad.$$

B. Dynamic Equilibrium Angle

The (10) is a liner differential equation due to the use of coefficients frozen method, and the analytic solution can be obtained after the roots to the following two equations, whose right terms are gravity term and control force term respectively.

1) Formula for dynamic equilibrium angle due to the gravity term

Consider the equation as follows:

$$\Delta'' + (H - iP)\Delta' - (M + iPT)\Delta = G \quad . \qquad (11)$$

Let $\Delta_0 = c_1 e^{l_1 s} + c_2 e^{l_2 s}$, and Δ_0 is a particular solution, so

$$l_1 + l_2 = -(H - iP), \quad l_1 l_2 = -(M + iPT).$$

Let $c_1' e^{l_1 s} + c_2' e^{l_2 s} = 0$ and differentiating Δ_0, it gives

$$c_{1,2}' = \pm\frac{G}{l_1 - l_2}e^{-l_{1,2}s} = \pm\frac{1}{l_1 - l_2}\frac{g\cos\varphi}{v^2}\left(k_{zz} - i\frac{J_{xf}\dot{\gamma}_f + J_{xa}\dot{\gamma}_a}{Av}\right)e^{-l_{1,2}s} \quad.$$

Let $Q^* = k_{zz} - i(J_{xf}\dot{\gamma}_f + J_{xa}\dot{\gamma}_a)/Av$. The quantity of Q^* is small [13], and the velocity changes slowly. Therefore Q^* is seen as a constant in a small period of time. Integrating the $c_{1,2}'$, we have

$$c_{1,2} = \pm\frac{gQ^*}{l_1 - l_2}\frac{1}{-l_{1,2}}\frac{\cos\varphi}{v^2}e^{-l_{1,2}s} \quad.$$

So a particular solution to (11) is

$$\Delta_{0g} = -\frac{g\cos\varphi}{v^2(M + iPT)}\left(k_{zz} - i\frac{J_{xf}\dot{\gamma}_f + J_{xa}\dot{\gamma}_a}{Av}\right) \quad. \qquad (12)$$

And when in the control process it gives

$$\begin{cases} \delta_{\alpha g} = \dfrac{g\cos\varphi}{v^2(M^2 + iP^2T^2)}\left(-k_{zz}M + \dfrac{J_{xa}\dot{\gamma}_a}{Av}PT\right), \\[3mm] \delta_{\beta g} = \dfrac{g\cos\varphi}{v^2(M^2 + iP^2T^2)}\left(\dfrac{J_{xa}\dot{\gamma}_a}{Av}M + k_{zz}PT\right). \end{cases}$$

$\delta_{\alpha g}$ and $\delta_{\beta g}$ are the components in vertical and horizontal plane.

2) Formula for dynamic equilibrium angle due to the control force term

Consider the equation as follows:

$$\Delta'' + (H - iP)\Delta' - (M + iPT)\Delta = D \quad . \qquad (13)$$

Using the same method, the particular solution to (13) gives as follows:

$$\Delta_{0c} = -\frac{(k_c - b_c k_{zz}) + i b_c(J_{xa}\dot{\gamma}_a)/(Av)}{M + iPT}\delta_z e^{i\gamma_f} \quad. \qquad (14)$$

3) Particular solution to the equation of attack angles

Let Δ be the general solution to (10), and we have

$$\Delta = C_1 e^{(\lambda_1 + i\phi_1)s} + C_2 e^{(\lambda_2 + i\phi_2)s} + \Delta_0 \quad, \qquad (15)$$

$p_{1,2} = \lambda_{1,2} + i\phi_{1,2}$ are roots to homogeneous equation.

From (15), we know that the motion of the attack angles is synthesizes of two periodic circular moments. Because the projectile meets the dynamic stability condition, the real parts of the roots are negative, and the two periodic circular movements will attenuate to disappear. Then only the particular solution Δ_0 leaves, and the motion of the projectile axe will be around Δ_0, which is the dynamic

equilibrium angle.

Taking superposition of the solutions to a linearity differential equation, a particular solution to (10) is shown as:

$$\Delta_0 = \Delta_{0g} + \Delta_{0c} = -\frac{g\cos\varphi}{v^2(M + iPT)}\left(k_{zz} - i\frac{J_{xf}\dot\gamma_f + J_{xa}\dot\gamma_a}{Av}\right)$$

$$-\frac{(k_c - b_c k_{zz}) + ib_c(J_{xa}\dot\gamma_a)/(Av)}{M + iPT}\delta_z e^{i\gamma_f} \quad . \tag{16}$$

Due to $\dot\gamma_f = 0$, we have

$$\Delta_{0k} = -\frac{g\cos\varphi}{v^2(M + iPT)}\left(k_{zz} - i\frac{J_{xa}\dot\gamma_a}{Av}\right)$$

$$-\frac{(k_c - b_c k_{zz}) + ib_c(J_{xa}\dot\gamma_a)/(Av)}{M + iPT}\delta_z e^{i\gamma_f} \quad . \tag{17}$$

IV. MECHANISM OF TRAJECTORY CORRECTION

Formula of the deviation motion is acquired firstly, which points out that the dynamic equilibrium angle induced by trajectory correction is the key factor. Then mechanism of trajectory correction and method of drift value are introduced.

A. Deviation Motion

The point mass trajectory model is the first order approximation of the real trajectory, and depends on the gravity as well as the zero yaw axial force. In the flight, other aerodynamic forces and moments act on the projectile, and make the flight contrail diverge from the particle trajectory. The motion perpendicular to the point mass trajectory is called the deviation motion [14].

Assuming that the components of the deviation motion are y_p and z_p, so we have

$$\ddot y_p + i\ddot z_p = \left(F_{y4} + iF_{z4}\right)/m$$

$$= \left(b_y + b_c + i\frac{b_{zf}\dot\gamma_f + b_{za}\dot\gamma_a}{v}\right)v^2\Delta - g\cos\varphi \quad . \tag{18}$$

Taking the arclength s as variable, it gives

$$y_p'' + iz_p'' = \left(b_y + b_c + i\frac{b_{zf}\dot\gamma_f + b_{za}\dot\gamma_a}{v}\right)\Delta - \frac{g\cos\varphi}{v^2} \quad . \tag{19}$$

Substituting (17) into (19), it gives

$$y_p + iz_p = \iint\left[\left(b_y + b_c + i\frac{b_{za}\dot\gamma_a}{v}\right)(\Delta_{0g} + \Delta_{0c}) - \frac{g\cos\varphi}{v^2}\right]\mathrm{d}s\,\mathrm{d}s$$

$$= \iint\left[\left(b_y + b_c + i\frac{b_{za}\dot\gamma_a}{v}\right)\Delta_{0g} - \frac{g\cos\varphi}{v^2}\right]\mathrm{d}s\,\mathrm{d}s$$

$$+ \iint\left[\left(b_y + b_c + i\frac{b_{za}\dot\gamma_a}{v}\right)\Delta_{0c}\right]\mathrm{d}s\,\mathrm{d}s \quad . \tag{20}$$

From (20), we get

$$y_C + iz_C = \iint\left[\left(b_y + b_c + i\frac{b_{za}\dot\gamma_a}{v}\right)\Delta_{0c}\right]\mathrm{d}s\,\mathrm{d}s \quad , \tag{21}$$

y_C and z_C are the position vector components caused by trajectory correction in vertical and horizontal plane.

B. Analysis of Correction Mechanism

Aiming to analyze the correction mechanism of the projectile, a step command is applied. That is to say the correction part stays in a fixed roll angle. Through this method, the angle motion is studied, and the correction mechanism is presented.

From (21) we know that Δ_{0c} is the key factor, and the algebraic symbols of its real part and imaginary part are the wsymbols of y_C and z_C, because

$$\left|b_y + b_c\right| \gg \left|\frac{b_{za}\dot\gamma_a}{v}\right| \quad .$$

After disposal of (14), it gives

$$\begin{cases}\delta_{\alpha c} = -\dfrac{\delta_z}{M^2 + P^2 T^2}\left(B_l\cos\gamma_f - B_h\sin\gamma_f\right) \quad , \\[2mm] \delta_{\beta c} = -\dfrac{\delta_z}{M^2 + P^2 T^2}\left(B_l\sin\gamma_f + B_h\cos\gamma_f\right) \quad .\end{cases} \tag{22}$$

where

$$\begin{cases}B_l = \left(k_c - b_c k_{zz}\right)M + PTb_c\dfrac{J_{xa}\dot\gamma_a}{Av} \quad , \\[2mm] B_h = Mb_c\dfrac{J_{xa}\dot\gamma_a}{Av} - \left(k_c - b_c k_{zz}\right)PT \quad .\end{cases}$$

$\delta_{\alpha c}$, $\delta_{\beta c}$ are the vertical and horizontal components of the dynamic equilibrium angle causing by the control force.

For the projectile researched in this paper, $B_l > 0$ and $B_h < 0$, so the sign of $\delta_{\alpha c}$, $\delta_{\beta c}$ is defined by the roll angle γ_f of the fixed canards. So it gives

$$\begin{cases}\gamma_f = 0, \ \delta_{\alpha c} < 0, \ \delta_{\beta c} > 0 \quad , \\ \gamma_f = 90, \ \delta_{\alpha c} < 0, \ \delta_{\beta c} < 0 \quad , \\ \gamma_f = 180, \ \delta_{\alpha c} > 0, \ \delta_{\beta c} < 0 \quad , \\ \gamma_f = -90, \ \delta_{\alpha c} > 0, \ \delta_{\beta c} > 0 \quad .\end{cases} \tag{23}$$

The causes of this phenomenon can be explained. Taking $\gamma_f = 0$ for example, when the projectile axis has the movement trend because of the control force, the axis will

deflect to the right immediately due to the gyroscopic effect of high speed rotating formation. After the total attack angle raise, the axis moves to the bottom right direction under the overturn moment acting. The overturn moment is perpendicular to the plane defined by the projectile axis and the velocity vector, and it takes the axis under the real axis. Although the projectile can move above the real axis, the average position is under the real axis.

By the (21), the deviation motion is the double integration of the attack and sideslip angle, which is the correction result of the control force. The drift value can be acquired by integration along the trajectory, so we can get the analysis result as follows:

$$
\begin{cases}
\gamma_f = 0, \ \Delta L < 0, \ \Delta H > 0 \ , \\
\gamma_f = 90, \ \Delta L < 0, \ \Delta H < 0 \ , \\
\gamma_f = 180, \ \Delta L > 0, \ \Delta H < 0 \ , \\
\gamma_f = -90, \ \Delta L > 0, \ \Delta H > 0 \ .
\end{cases}
$$

where ΔL and ΔH are the correction values along the longitudinal and lateral direction.

C. Drift Value Computing

Deducing the two right terms of (20) respectively, it gives

$$
P_{p1} = \frac{\left[b_y + b_c + i\left(b_{zf}\dot{\gamma}_f + b_{za}\dot{\gamma}_a \right)/v \right]}{M + iPT}
$$

$$
\times \left(-k_{zz} + i\frac{J_x\dot{\gamma}_f + J\dot{\chi}_a}{Av} \right) \iint \frac{g\cos\varphi}{v^2} ds ds \ , \qquad (24)
$$

$$
P_{p2} = \iint \left[\left(b_y + b_c + i\frac{b_{zf}\dot{\gamma}_f + b_{za}\dot{\gamma}_a}{v} \right)\Delta_{0c} \right] ds ds \ . \qquad (25)
$$

P_{p1}, P_{p2} mean the deviation motions caused by the gravity and control force terms. From P_{p1}, P_{p2}, we get the drift formulas causing by the gravity and control force terms as follows:

$$
z_{p1} = X_L \left(|\varphi_{im}| + \varphi_0 \right) \frac{J_{xa}\dot{\gamma}_a}{MAv} \left(b_y + b_c \right) \ , \qquad (26)
$$

$$
z_{p2} = -\frac{\delta_z \left(v_{im}^2 - v_0^2 \right)}{2gb_x M} \ln \frac{\sec\varphi_{im} + \tan\varphi_{im}}{\sec\varphi_0 + \tan\varphi_0}
$$

$$
\times \left[\left(D_l M + D_h PT \right)\sin\gamma_f + \left(D_h M - D_l PT \right)\cos\gamma_f \right] \ . \qquad (27)
$$

where

$$
\begin{cases}
D_l = \left(b_y + b_c \right)\left(k_c - b_c k_{zz} \right) - b_c \dfrac{b_{za}\dot{\gamma}_a}{v} \dfrac{J_{xa}\dot{\gamma}_a}{Av} \ , \\
D_h = \left(k_c - b_c k_{zz} \right)\dfrac{b_{za}\dot{\gamma}_a}{v} + \left(b_y + b_c \right)b_c \dfrac{J_{xa}\dot{\gamma}_a}{Av} \ .
\end{cases}
$$

z_{p1}, z_{p2} are on behalf of the draft values of the gravity and control force terms. We can calculate the drift values in small periods, then can get the drift values along the trajectory due to gravity and control force through integration. The value of trajectory drift is acquired by the summation of the two.

V. NUMERICAL EXAMPLE

This paper takes a certain large caliber projectile as an example. The trajectory model and aerodynamic coefficients have been checked by flight experiments, and the initial conditions of the experiments were shown in TABLE I.

The simulation result of the free flight is shown in Fig. 3. The flight of the projectile lasts 69.83 s, and the range and deflection are 19307.6 m and 686.1 m respectively.

TABLE I
Simulation initial conditions

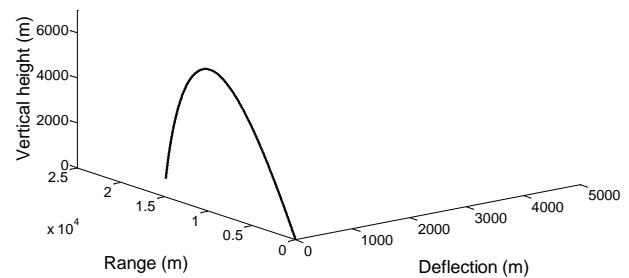| Mass / kg	Muzzle velocity / (m/s)	Spin rate of body / (r/s)
45.5	650	210
Elevation / °	Altitude / m	Spin rate of canards / (r/s)
45	1426	-10

Fig. 3. Simulation results under no control condition

Using the initial conditions shown in TABLE I, some simulations are conducted under control state. The correction starts at 10 s after the projectile is fired, and the control angle would be the same value until the projectile is impacted.

For example, the control angle is $0°$. The drift values caused by the gravity and control force are in TABLE II where z_{p1} and z_{p2} mean the draft values. The largest values

are obtained when the projectile is near the top point of the trajectory, and the period is 30～40s, and the drift value computed using the coefficient frozen method is 703.85 m. The simulation drift value is 716.7 m. The error between the two values is 12.85 m, which is in the error range. The results in Tab. 2 show the effectiveness of the formula deducing process.
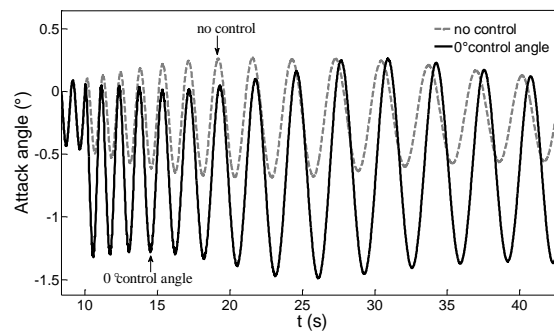
The curves of the attack and sideslip angle are shown in Fig. 4. Fig. 4 a) shows that the average value of the attack angle depressed 0.5° compared to the no control condition after the course correction begins, and in Fig. 4 b) the average value of sideslip angle depresses 0.1°. TABLE Ⅱ and Fig. 4 indicate that the average position of the projectile axis comes to the reverse direction, and will produce correction in the opposite direction.

TABLE Ⅱ
DRIFT VALUES UNDER CONTROL STATE

Periods / s	z_{p1} / m	z_{p2} / m
0～10	95.54	--
10～20	122.52	-11.84
20～30	144.25	-14.68
30～40	147.07	-15.82
40～50	127.59	-15.12
50～60	97.22	-13.64
60～69.6	48.31	-7.55
	782.5	-78.65
summation	703.85	

Considering the general cases, the control angle can be set at any position. For example, set the control at -45°, and the changes of the attack and sideslip angle are shown in Fig. 5. The projectile axis moves to the down direction in the vertical plane, and to the right direction in the horizontal plane. The results coincide with the theoretical analysis in section IV.

In order to prove the analysis of the correction mechanism, TABLE Ⅲ shows the results under different control angles. It gives that the components of the control angle in vertical and horizontal plane would produce motion of the projectile and trajectory correction. But the trajectory correction value is in the opposite direction.
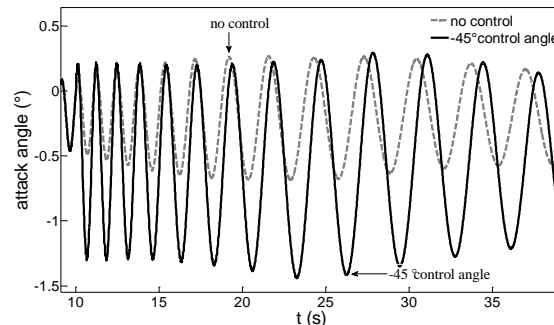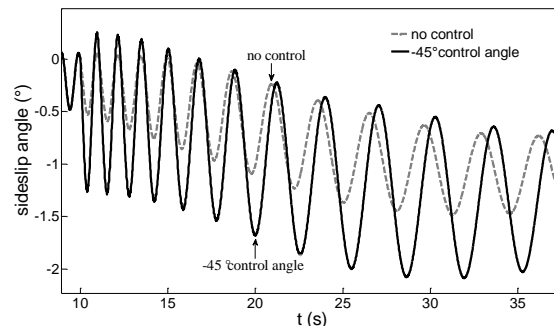

a) Curves of the attack angle
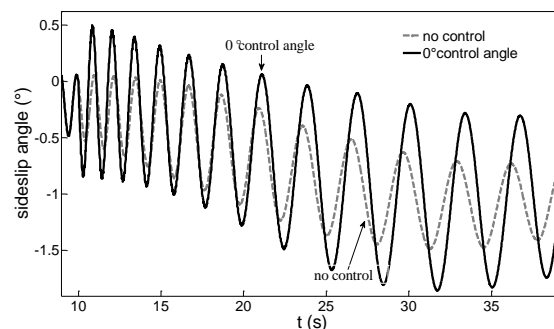
b) Curves of the sideslip angle

Fig. 4. Curves of attack angle and sideslip angle when the control angle is 0°

a) Curves of the attack angle

b) Curves of the sideslip angle

Fig. 5. Curves of attack angle and sideslip angle when the control angle is -45°

TABLE Ⅲ
SIMULATION RESULTS UNDER DIFFERENT CONTROL ANGLES

Condition	Control angle/ °	Range/m	deflection/m
No control	-	19361	691
Control	0	19228.6	726.7
	45	19268	652
	90	19362	625
	180	19431	615
	-90	19252.9	788.5
	-45	19326	774.582

VI. CONCLUSION

This work presented the correction mechanism of a class of spin stabilized projectiles with fixed canards. Formulas of dynamic equilibrium angle and drift were deduced. By studying the angle motion of the projectile axis under control state, the mechanism was explored. The components of control angle in the vertical and horizontal planes make the projectile axis move to the angle opposite directions of components in corresponding plane, which make the forces and moments change. It gives that if the components value of the control angle is positive, the projectile axis moves to the opposite direction, and negative correction value of the impact point occurs.

REFERENCE

[1] Regan F., Smith J., "Aeroballistics of a terminal correction spinning projectile (TCSP)," *AIAA Mechanics and Control of Flight Conference*, Anaheim, Calif., Vol. 12, NO. 12, 1975, pp. 733-738.

[2] Yang C., Lin C., Chopper K., et al, "Analysis and evaluation of guidance integrated fuzing," *AIAA-93-3786CP*, pp. 80 –808.

[3] Wernert P., Theodoulis S., "Modeling and stability analysis for a class of 155 mm spin-stabilized projectiles with course correction fuse(CCF)," *AIAA Atmospheric Flight Mechanics Conference and Exhibit*, Portland Oregon, 2011, pp. 1-13.

[4] Wernert P., "Stability analysis for canard guided dual-spin stabilized projectiles," *AIAA Atmospheric Flight Mechanics Conference*, Chicago, 2009, pp. 1-24.

[5] Theodoulis S., Gassmann V., Wernert P.. Guidance and control design for a class of spin-stabilized fin-controlled projectiles," *Journal of Guidance, Control and Dynamics*, Vol. 36, NO. 2,2013, pp. 517-531.

[6] WANG Z. Y., CHANG S. J., "Impact point prediction and analysis of lateral correction analysis of two-dimensional trajectory correction projectiles", *2013 9th International Conference, China Ordnance Society on Defence Technology*, pp. 48-52.

[7] Costello M., "Modeling and simulation of a differential roll projectile," *Proceedings of the 1998 AIAA Modeling and Simulation Technologies Conference*, Boston, MA, 1998, pp. 490-499.

[8] Costello M., Allen Peterson, "Linear theory of a dual-spin projectile in atmospheric flight," *Journal of Guidance, Control and Dynamics*, Vol. 23, NO. 5, 2000, pp. 789-797.

[9] JI X. L., WANG H. P., ZENG S. M., "CFD Prediction of longitudinal aerodynamic for a spinning projectile with fixed canard," *Transactions of Beijing Institute of Technology*, Vol. 31, NO. 3, 2011, pp. 265-268.

[10] ZHANG J. Y., WANG G, HAO Y. P., "The investigation of aerodynamic characteristics for two-dimensional trajectory correction projectile canard rudder device," *Journal of Projectiles, Rockets, Missiles, and Guidance*, Vol. 33, NO. 2, 2013, pp. 88-91.

[11] LI W., WANG Z. G., "Analysis of motion characteristic for dual-spin projectile," *Journal of Solid Rocket Technology,* Vol. 37, NO. 2, 2014, pp. 143-149.

[12] Toledo W., Recchia T., Su W., et al, "Aeroballistics diagnostics fuse (DFuse) analysis of a 120mm mortar munition," *AIAA Infotech @ Aerospace Conference*, Seattle, Washington, 2009, pp. 1-11.

[13] HAN Z. P., et al, "Exterior ballistics of rockets and projectiles," *Beijing Institute of Technology Press*, Beijing, 2008, pp. 150-153.

[14] Murphy, C.H., "Free flight motion of symmetric missiles," *US Army Research Lab*. Rept. 1216, Aberdeen Proving Ground, MD, 1963.